



Original Research Article

## In Situ Catalytic Conversion of Glycerol to Triacetin under Microwave Irradiation with Commercial Palladium on Activated Carbon Catalyst

Nadzirah Azmi<sup>1</sup>, Mariam Ameen<sup>2</sup>, G. Yashni<sup>3</sup>, Suzana Yusup<sup>4</sup>, Mohd Hizami Mohd Yusoff<sup>1</sup>, Yee Ho Chai<sup>\*1</sup>

<sup>1</sup>HICoE – Biomass Processing Lab, Centre of Biofuel and Biochemical Research, Institute of Self-Sustainable Building, Department of Chemical Engineering, Universiti Teknologi PETRONAS, 32610 Bandar Seri Iskandar, Perak, Malaysia

e-mail: [nadzirah\\_21000025@utp.edu.my](mailto:nadzirah_21000025@utp.edu.my), [hizami.yusoff@utp.edu.my](mailto:hizami.yusoff@utp.edu.my), [yecho.chai@utp.edu.my](mailto:yecho.chai@utp.edu.my)

<sup>2</sup>School of Chemical and Environmental Engineering, RMIT University Melbourne 3000 Victoria, Australia  
e-mail: [mariam.ameen@rmit.edu.au](mailto:mariam.ameen@rmit.edu.au)

<sup>3</sup>Faculty of Engineering and Computer Technology, AIMST University, 08100 Bedong, Kedah, Malaysia  
e-mail: [yashni\\_g@yahoo.com](mailto:yashni_g@yahoo.com)

<sup>4</sup>Generation Unit, Fuel and Combustion Section, TNB Research Sdn. Bhd., Selangor, Malaysia  
e-mail: [drsuzanayusuf@yahoo.com](mailto:drsuzanayusuf@yahoo.com)

Cite as: Azmi, N., Ameen, M., Yashni, G., Yusup, S., Mohd Yusoff, M. H., Chai, Y. H., In Situ Catalytic Conversion of Glycerol to Triacetin under Microwave Irradiation with Commercial Palladium on Activated Carbon Catalyst, *J.sustain. dev. energy water environ. syst.*, 11(4), 1110465, 2023, DOI: <https://doi.org/10.13044/j.sdewes.d11.0465>

### ABSTRACT

The depletion of non-renewable fossil fuels has increased the importance of carbon-neutral resources like biofuel and biodiesel. Biodiesel is a better fuel option than petrodiesel due to its excellent lubricity, non-toxic nature, and lack of sulphur. However, the excess production of glycerol is a challenge for biodiesel usage. This study investigates using an acetylation process with palladium on the activated carbon catalyst to convert glycerol into triacetin, a potential fuel additive for biodiesel blends. The study optimises the reaction parameters using response surface methodology to achieve high selectivity for triacetin. The study determined that the optimised parameters for achieving 96.64% glycerol conversion and 0.231% triacetin selectivity are 110 °C, a 1:10 glycerol-acetic acid mole ratio, and 0.718 wt% catalyst loading. Analysis of variance revealed that the reaction temperature significantly impacts glycerol conversion, while the glycerol-acetic acid mole ratio affects the selectivity of triacetin.

### KEYWORDS

*Glycerol, Activated carbon, Acetylation, Triacetin, Microwave-assisted reaction.*

### INTRODUCTION

The growth of the biodiesel industry has been increasing rapidly in recent years. Approximately 85 million barrels per day (Mb/d) or 3900 million metric tonnes of oil equivalent (Mtoe) were produced globally in 2010 [1]. The experts predict that future oil production will be around 300 Mb/d by 2100 [2]. Whereas biodiesel production in Malaysia has increased at an average annual rate of 36.41% from zero barrels per day to 29.12 thousand barrels per day between 2000 and 2019, owing to increased demand for local usage and exports [3].

Despite the accelerated progress in the formulation and production of biodiesel, numerous challenges are evolving, and these must be tackled competently. One of the main challenges is

\* Corresponding author

the unavoidable low-value generation of glycerol (glycerine/1,2,3-propanetriol) as a by-product of biodiesel from the transesterification process [4]. For every biodiesel production, 10 wt% of glycerol is generated based on stoichiometric reaction balance [5]. Glycerol's global market, estimated to be 2.8 million metric tonnes in 2020, is expected to increase to 4 million metric tonnes in 2027 [6]. Between 2015 and 2019, the value of Malaysian glycerol increased by 1%, while the quantity increased by 3% annually [7]. This excessive glycerol must be converted into value-added chemicals [8], preferably into high-value-added products such as chemicals, oxygenated fuel additives, solvents, and polyesters. Glycerol can produce esters of glycerol such as monoacetin (MAG), diacetin (DAG), and triacetin (TAG) via acetylation with acetic anhydride, ethyl acetate, and acetic acid in the presence of appropriate catalysts [9]. Acetylation of glycerol to produce acetins garnered wide interest from researchers owing to its various applications for the end products, such as a solvent for dyes, plasticisers, etc.

Furthermore, acetins demonstrate exceptional capabilities as fuel additives to decrease carbon monoxide emissions, particulate matter, unburned hydrocarbon emissions, and unregulated aldehydes. They have great potential for enhancing cold flow properties and reducing viscosity when introduced into formulations of diesel and biodiesel [10]. They can also be used as plasticisers of cellulosic polymers and copolymers, antiknock additives for gasoline, and in manufacturing explosives and biodegradable polyesters [8]. Moreover, they are widely utilised as food additives, solvents in leather tanning industries, and the manufacture of cigarette filters [11].

Conventional approaches for the industrial manufacture of triacetin typically require a longer time of reaction and operate at high temperatures. Hence, applying catalysts is recommended to attain a less energy-intensive and lower-temperature process [12]. Therefore, this research focuses on transforming glycerol into high-value products through acetylation to produce triacetin as an economically feasible alternative. Acetylation is the direct esterification between glycerol and acetic acid or acetic anhydride in the presence of appropriate acid catalysts [5]. Over numerous types of catalysts, acetic anhydride as the acetylating agent optimises the reaction with 100% glycerol conversion and more than 90% triacetin selectivity in a shorter reaction time. Nonetheless, this approach is unsuitable because acetic anhydride is more expensive than acetic acid; the reaction is extremely exothermic and risks human health [4]. While some investigators have shown reduced selectivity with acetic acid, few have reported increased triacetin selectivity when using excessive acetic acid to address this constraint [11].

Recently, numerous catalysts have been synthesised and investigated for the acetylation of glycerol with acetic acid. Homogeneous catalysts such as sulphuric acid ( $H_2SO_4$ ), hydrochloric acid (HCl), or phosphoric acid ( $H_3PO_4$ ) were used for the acetylation of glycerol. Homogeneous catalysts have a few key drawbacks. Firstly, it is challenging to separate these catalysts effectively, often necessitating the use of neutralisation agents. Secondly, they can cause corrosion problems for the equipment involved. Lastly, using homogeneous catalysts produces significant hazardous waste [13].

Moreover, using homogeneous catalysts is frequently related to insufficient reusability, environmental threats, and reduced purity of the main product [9]. The workaround solution involves using heterogeneous catalysts, which provide multiple benefits, including improved selectivity for desired products, lower toxicity, easy separation, and reusability, unlike homogeneous catalysts [14]. Hence, various studies focused on the development of different types of heterogeneous catalysts such as zeolites [15], heteropoly acids [16], Amberlyst 15 [17], cobalt oxide on tin oxide [18], and ruthenium/copper nanoparticles in mesoporous silica derived from rice husk ash [19] for the esterification of glycerol with acetic acid. However, the selectivity of triacetin is limited for several reasons. These include the decreasing acidity of the catalysts, the successive acetylation of hydroxyl groups, restricted access to acidic sites, the presence of water, and narrow pores. [20]. These gaps allow the researchers to implement different types of solid acid catalysts to substitute for the existing catalyst.

Using carbon-based catalysts for glycerol acetylation shows great promise, as carbon is stable in both acidic and basic environments. This stability makes carbon an attractive choice for glycerol acetylation. Okoye *et al.* have performed glycerol acetylation using the synthesised glycerol-based carbon catalyst [21]. This acetylation reaction converted 99% of the glycerol and produced 88% DAG and TAG. Furthermore, using metal support on activated carbon improves the catalytic activity and selectivity of the targeted compound [22]. Moreover, the doped metal on activated carbon can further maximise its surface area, which can enhance the activity of the catalysts during the esterification reactions [23].

Because of its structural similarity to graphite, AC can be functionalised with groups such as SO<sub>3</sub>H, Ph-SO<sub>3</sub>H, and so on, just like graphite, fullerenes, nanotubes, or graphene [24]. Researchers used this feature to create sulphonated-active carbons (ACs) with -SO<sub>3</sub>H groups. Sulphonated activated carbons are highly researched catalysts anticipated to replace concentrated H<sub>2</sub>SO<sub>4</sub> in industries. When utilised as solid acids, they have demonstrated the ability to catalyse various reactions, including cellulose hydrolysis, esterification, nitration, and transesterification [25].

Palladium (Pd) is one of the noble metals that can be active under both acidic and alkaline conditions [26]. Besides, palladium on activated carbon (Pd/AC) catalyst is one of the most widely utilised commercial catalysts in the catalytic process due to its higher catalytic activity and selectivity. Therefore, in this study, Pd/AC was investigated as a solid acid catalyst for glycerol acetylation.

Microwave-assisted heating is an advanced technique in organic reactions that offers shorter reaction times. In contrast, conventional heating methods using a coil or jacket recirculation do not evenly distribute heat throughout the system. In this context, the reaction medium takes longer to reach the desired temperature and often experiences uneven heat distribution due to conduction and convection in conventional heating methods. However, microwave radiation interacts directly with the system without interfering with the molecules in the reaction mixture, eliminating these issues [27].

Microwave irradiation is a process that delivers evenly distributed heating to a reaction medium [28]. Furthermore, microwave-assisted reaction is an easy, clean, and effective method compared to conventional heating [15]. Considering the previously reported findings in the literature, limited research has been done using microwaves in glycerol acetylation using Pd/AC. With the potential of the Pd/AC catalyst as an active catalyst and the ability of microwave irradiation to shorten the reaction time, this research can bridge the gap in the acetylation of the glycerol process. Hence, this underlines the novelty of the present work.

## MATERIALS AND METHODS

Acetic acid (purity > 99.85%), glycerol (purity > 99.9%), and palladium on activated carbon (5 wt% Pd) were obtained from Sigma Aldrich Company and utilised without further purification. Triacetin standard (>99.0%) was purchased from Sigma Aldrich (Germany).

### Characterisation of palladium on activated carbon

The surface morphology, textural properties, and elemental compositions of the Pd/AC catalyst were studied using Field Emission Scanning Electron microscopy coupled with Energy-Dispersive Spectroscopy (FESEM-EDS; ZEISS SUPRA 35VP) [21].

The thermal stability of Pd/C was analysed using a thermal gravimetric analyser (TGA; Mettler Toledo 851e, Switzerland) at a temperature range of 50 to 600 °C. The heating rate was 10 °C/min in a continuous nitrogen gas flow at 50 mL/min [4].

X-ray diffraction (XRD) patterns of Pd/AC were analysed on a Bruker JDX 8030 phaser using Copper K $\alpha$  radiation ( $\lambda = 0.15406$  nm) with a  $2\theta$  range of 2–80° with a step size of 0.02° [29].

NH<sub>3</sub>-temperature-programmed desorption (NH<sub>3</sub>-TPD) was used to determine the surface acid site density and acid strength of Pd/AC (Micromeritics Autochem II 2920 chemisorption analyser).

The catalyst was evacuated with helium at a rate of 20 mL/min from the surrounding temperature to 150 °C for 1 hour, then cooled to 40 °C, and 15% NH<sub>3</sub> gas was absorbed by the Pd/AC catalyst for 1 hour at a rate of 20 mL/min. [14].

Using a Bruker Alpha spectrometer and the attenuated total reflection (ATR) method, a Fourier transform infrared spectrometer (FTIR) was utilized to analyse the surface and functional groups over a wavenumber range of 400 to 4000 cm<sup>-1</sup> [21].

### Experimental setup

The acetylation of glycerol reactions using acetic acid was conducted in a 250 mL three-necked round bottom flask in a microwave reactor setup, as shown in Figure 1. Chill water continuously flows through the condenser coil to prevent the evaporation of reactants under atmospheric pressure.

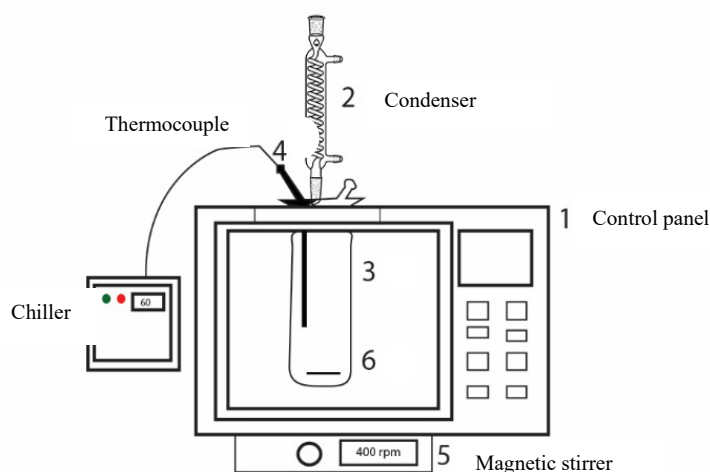


Figure 1. Schematic diagram of experimental equipment [15]

Firstly, a fixed amount of Pd/AC catalyst and glycerol (Table 1) were mixed in a 100 mL beaker. Acetic acid was measured and poured out separately in a 100 mL beaker. The Pd/AC catalyst and glycerol mixture, followed by acetic acid, was transferred to a 250 mL three-necked round-bottom flask. The reaction flask was then placed into the microwave chamber. The reaction was started initially at a low micropower setting. The reaction was run for 90 min and continuously stirred using a magnetic stirrer at 400 rpm. At the end of the reaction, the mixture was cooled to room temperature and filtered to separate the Pd/AC catalyst from the reactant. The mixture of the reactant was then transferred to a sampling bottle and stored for triacetin analysis using gas chromatography with flame ionisation detection (GC-FID) analysis as described and high-performance liquid chromatography (HPLC) for glycerol conversion [9].

### Product analysis

The liquid product from acetylation of glycerol was analysed by gas chromatography (GC, Agilent 7820A with autosampler 7683) equipped with a flame ionisation detector (FID) and a capillary column (HP-5, 30 m×0.32 mm, 0.25 μm). Helium was used as a carrier gas at 25 mL/min. The injector and detector were set at 280 °C and 320 °C, respectively. External calibration for triacetin standard samples was prepared. Samples were prepared by mixing 700 μL of ethanol (GC grade) with 500 μL of the product as the internal standard. Firstly, 1 μL of the sample was injected at 70 °C, then increased up to 270 °C at the rate of 70 °C/min and detained for 2 min, and finally increased to 300 °C at the rate of 20 °C/min. Triacetin was detected based on its retention times using the GC-FID, which was pre-calibrated and determined by relative peak areas [9]. The glycerol conversion was determined by HPLC using an Agilent Hi-Plex H column (7.7 × 300 mm,

8  $\mu\text{m}$ ) at 65 °C under an oven with mobile phase 0.005 M sulphuric acid and a flow rate of 0.6 mL/min using a refractive index detector. The external calibration curve was prepared for glycerol conversion [30].

### Experimental design for optimisation of the acetylation of glycerol

Each Central Composite Design (CCD, Design-Expert® version 10 software) was used to design the independent factors that affect the acetylation of glycerol. **Table 1** shows the list of the variables and their ranges used for this analysis. Fifteen experimental runs were constructed, with one run anticipated to authenticate the effectiveness of the measured parameters on the results. The three independent factors include temperature (80–110 °C), acetic acid: glycerol mole ratios (5–10), and Pd/AC catalyst loadings (0.5–2.5 wt%) using three levels for each factor. Two dependent variables were assessed after each experimental run.

Table 1. Design parameters for acetylation of glycerol using a Pd/AC catalyst

Name	Unit	Low	High	-alpha	+alpha
Temperature	°C	80	110	73.7868	116.213
Molar ratio		5	10	3.96447	11.0355
Catalyst loading	%	0.5	2.5	0.0857864	2.91421

The glycerol conversion and the triacetin selectivity were determined using eq. (1) and eq. (2):

$$\text{Glycerol conversion, } GC [\%] = \frac{\text{Moles of converted glycerol}}{\text{Moles of initial glycerol}} \times 100 \quad (1)$$

$$\text{Triacetin selectivity, } TS [\%] = \frac{\text{Moles of triacetin produced}}{\text{Mole of glycerol reacted}} \times 100 \quad (2)$$

### Statistical analysis

The importance of the independent factors and the correlation between these parameters were analysed using ANOVA ( $p < 0.05$ ). The role of the independent factors in the acetylation of glycerol as a function of the quadratic model was determined by the adjusted coefficient of determination ( $R^2$  Adj.). Moreover, the relationship between the independent factors and their effect on the acetylation of glycerol was represented in three-dimensional (3D) graphical plots of response surface methodology (RSM).

RSM is crucial in examining the relationships between multiple variables and optimising complex processes. By utilising RSM, the response of a system to various experimental factors can be effectively analysed, and mathematical models can be derived to represent the relationship between these factors and the response variable. It enables the identification of optimal process conditions and the prediction of responses within a defined experimental space. Overall, statistical analysis using RSM enhances the understanding of complex systems and aids in optimising processes by providing valuable insights into the interactions and effects of multiple variables.

## RESULTS AND DISCUSSION

The external morphology of the Pd/AC is presented in **Figure 2**. The results revealed that the Pd/AC catalyst particles had non-uniform shapes. The EDX results of the Pd/AC composition are shown in **Table 2**. The EDX spectra confirmed the presence of the chemical constituents for Pd/AC as, in weight per cent, Pd = 1.96%, C = 97.04%, Si = 0.67%, and Cl = 0.34% and atomic per cent, Pd = 0.23%, C = 99.36%, Si = 0.29%, and Cl = 0.12%. The diffraction peaks' strong intensity and narrow width for Pd/AC indicate highly crystalline particles. However, the presence of other elements, such as Si and Cl, in the EDX spectrum

shows the occurrence of impurities, as the Pd/AC catalyst used in this investigation was a commercially available catalyst.

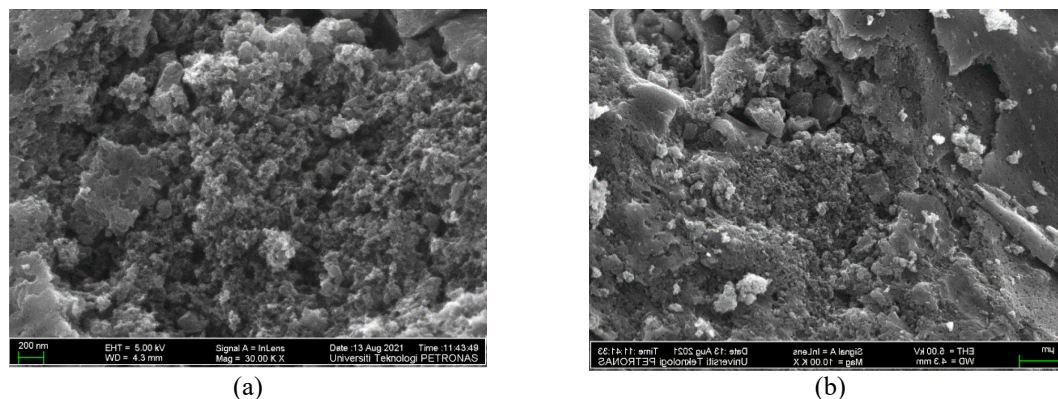


Figure 2. FESEM images of Pd/AC at 200 nm (a) and 1 μm magnification (b)

Table 2. Elemental composition of the catalysts

Component	Weight [%]	Atomic [%]
Carbon	97.03	99.36
Palladium	1.96	0.23
Silicon	0.67	0.29
Chloride	0.34	0.12

The thermal decomposition of the Pd/AC catalyst was investigated by TGA, as shown in **Figure 3**. The catalyst exhibited two major weight losses. The first weight loss was detected in the 80–90 °C range, and the second between 390–500 °C. The first weight loss below 100 °C is attributed to the loss of moisture or water molecules and the disintegration of small-molecule end-groups such as C–N, C–H, and C=O. The second weight loss is attributed to decomposing functional groups in Pd/AC. It designates the high stability of the Pd/AC catalyst and could be utilised at a temperature below 250 °C [20].

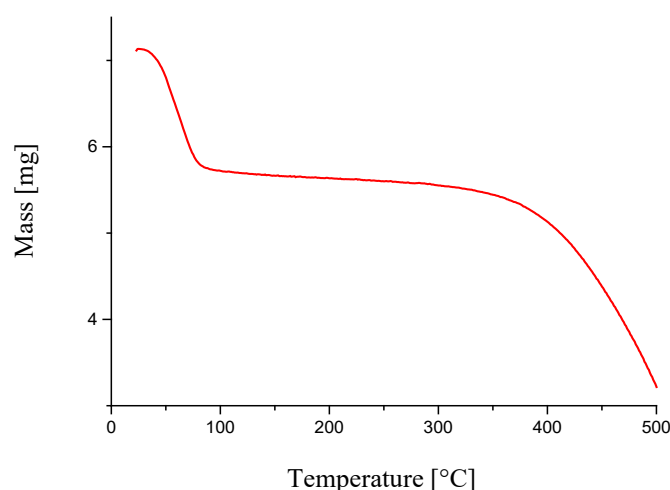


Figure 3. TGA profile of Pd/AC

XRD was used to analyse the composition and phase purity of the Pd/AC. XRD patterns of Pd/AC are presented in **Figure 4**, showing diffraction peaks with  $2\theta$  values at  $21.24^\circ$ ,  $26.95^\circ$ ,  $34.42^\circ$ ,  $40.49^\circ$ ,  $47.04^\circ$ ,  $50.49^\circ$ , and  $68.52^\circ$ . The broad band observed between  $20\text{--}30^\circ$  is characteristic of amorphous materials, which confirms that Pd/AC has a low degree of crystallinity with hexagonal graphite [22]. These are associated with  $sp^2$ -bonding carbon deficient in periodicity in the C-axis. The presence of Pd does not alter the structure of the AC and will not affect its resistance to high-temperature reactions [22]. The diffraction peaks at  $26.95^\circ$  and  $47.04^\circ$  are attributed to the carbon structure of activated carbon. The main peak at  $40.49^\circ$  suggested that a crystal phase was formed [31]. The presence of Pd in the samples caused weaker peaks of activated carbon. Besides, it is well acknowledged that the X-ray patterns of metal species are not detected as metals are vastly disseminated on the support [29].

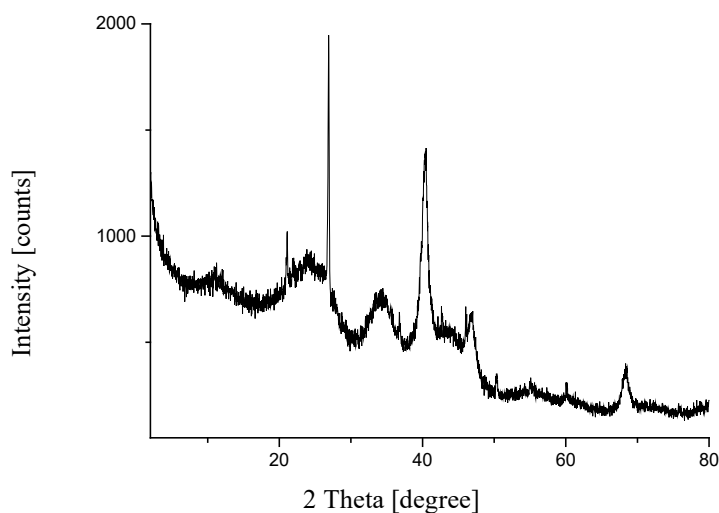


Figure 4. XRD patterns of Pd/AC

$\text{NH}_3$ -TPD results for the Pd/AC are shown in **Figure 5**. Two notable desorption peaks occur between  $760$  and  $740^\circ\text{C}$  and around  $840^\circ\text{C}$ , which are strong medium acid strength regions. The first desorption peak is ascribed to functional groups such as  $-\text{COOH}$  and  $-\text{OH}$ . The second peak is linked with the decomposition of carbon materials, including desorption of the  $-\text{CO}$  surface with phenolic and carbonyl functional groups. The Pd/AC also showed high acid site density, offering a sufficient anchoring site for the reaction of the acetylation of glycerol [20].

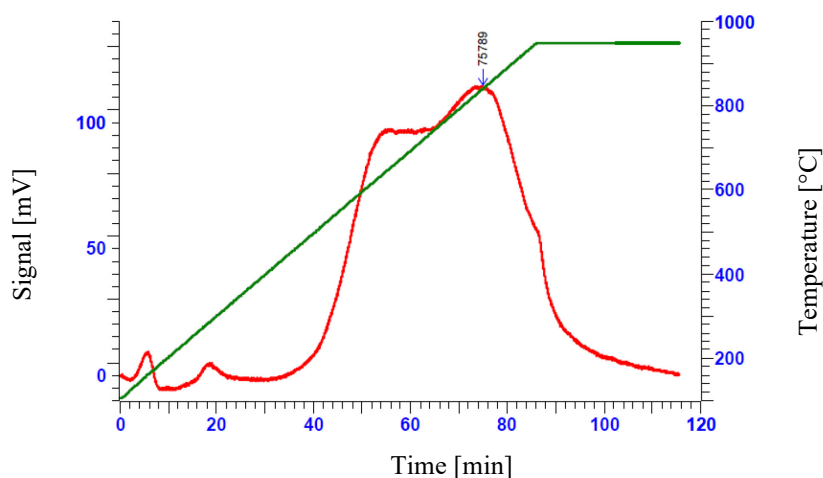


Figure 5.  $\text{NH}_3$ -TPD of Pd/AC

The FTIR spectrum of Pd/AC is depicted in **Figure 6**. The peaks were detected at  $1581.95\text{ cm}^{-1}$  and  $1224\text{ cm}^{-1}$ , representing the stretching vibrations of C=O and C=C and the bending vibration of the C–O–C groups, respectively [32]. C=C bonds in activated carbons are undoubtedly observed within the wavenumber range of  $1700\text{ cm}^{-1}$  to  $1600\text{ cm}^{-1}$  [33]. The peak at  $1091.79\text{ cm}^{-1}$  is related to C–O stretching vibrations, while the peak at  $2345.99\text{ cm}^{-1}$  is associated with C–H stretching vibrations. The intense band at  $3422\text{ cm}^{-1}$  is due to the stretching vibrations of –OH groups. Similarly, Ya'Aini *et al.* [33] observed the peaks of Pd/AC around  $3648\text{ cm}^{-1}$  and  $1200\text{ cm}^{-1}$ , typically due to the presence of hydroxyl and C–O groups, respectively. Moreover, they also detected a band at  $1550\text{ cm}^{-1}$ , possibly due to the stretching vibration C=O in the carboxyl, aldehyde, and ketone groups.

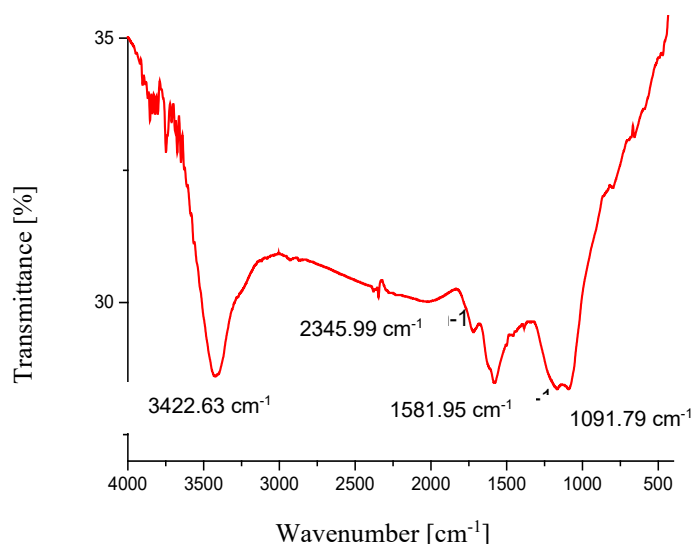


Figure 6. FTIR spectrum of Pd/AC

### Optimisation of the acetylation of glycerol

The optimisation of parameters for the glycerol acetylation using Pd/AC as the catalyst was conducted using Design-Expert software Version 12.

Table 3. Experimental design with triacetin selectivity and glycerol conversion

Run	Factor 1 <i>A</i> : Temperature [°C]	Factor 2 <i>B</i> : Molar ratio [-]	Factor 3 <i>C</i> : Catalyst loading [%]	Response 1 Triacetin selectivity [%]	Response 2 Glycerol conversion [%]
1	95	7.5	1.5	0.028	96.53
2	110	10	0.5	0.220	96.65
3	110	5	2.5	0.193	96.53
4	80	5	0.5	0.000	96.43
5	95	11.04	1.5	0.021	96.62
6	80	10	2.5	0.000	96.54
7	95	3.96	1.5	0.000	96.44
8	95	7.5	1.5	0.043	96.54
9	95	7.5	1.5	0.040	96.54
10	95	7.5	1.5	0.024	96.53
11	73.79	7.5	1.5	0.000	96.50
12	95	7.5	2.91	0.019	96.53
13	95	7.5	0.09	0.022	96.52
14	95	7.5	1.5	0.033	96.53
15	116.21	7.5	1.5	0.463	96.54



The maximum value for the glycerol conversion of 96.65% was recorded at Run 2. In contrast, the maximum triacetin selectivity was 0.463% at Run 15 (Table 3). Glycerol acetylation is an acid-catalysed reaction that needs acid sites with adequate strength [32]. The synthesis of triacetin through acetylation includes the transfer of a proton from the Pd/AC catalyst, which activates the carbonyl group of acetic acid and results in an elevated positive charge. The oxygen molecule of glycerol will attack the protonated acetic acid, which leads to the formation of monoacetin with the loss of one water molecule. The formed monoacetin was then further broken down into diacetin and triacetin in a sequence of reactions [9].

### Analysis of variance

According to the response surface methodology model fit, the quadratic model had the best fit in defining the impacts of parameters on triacetin selectivity. Table 4 shows the summary of the analysis of variance for the regression model for triacetin selectivity. The Model F-value of 286.22 implies the model is significant. In this case, temperature (*A*), molar ratio (*B*), catalyst loading (*C*), enhanced temperature parameter (*A*<sup>2</sup>), enhanced molar ratio (*B*<sup>2</sup>), and enhanced catalyst loading (*C*<sup>2</sup>) are significant model terms as the probability (*p*) values are less than 0.0500. Values greater than 0.1000 indicate the model terms are not significant. The Lack of Fit F-value of 2.98 implies the Lack of Fit is non-significant relative to the pure error. There is a 15.93% chance that a Lack of Fit F-value this large could occur due to noise. A non-significant lack of fit is good, which means it suits the model. Besides, the model's high R<sup>2</sup> value (0.9981) shows that the data is evaluated accurately. The Predicted R<sup>2</sup> of 0.9089 is in reasonable agreement with the Adjusted R<sup>2</sup> of 0.9946, where the difference is less than 0.2.

Table 4. Analysis of variance for the regression model for triacetin selectivity

Source	Sum of Squares	df	Mean Square	F-value	p-value	
Model	0.2252	9	0.0250	286.22	< 0.0001	significant
<i>A</i> – Temperature	0.1071	1	0.1071	1225.81	< 0.0001	significant
<i>B</i> – Molar ratio	0.0002	1	0.0002	2.56	0.1703	not significant
<i>C</i> – Catalyst loading	2.307E-06	1	2.307E-06	0.0264	0.8773	not significant
<i>AB</i>	0.0001	1	0.0001	0.8831	0.3905	not significant
<i>AC</i>	5.209E-07	1	5.209E-07	0.0060	0.9414	not significant
<i>BC</i>	0.0073	1	0.0073	83.48	0.0003	significant
<i>A</i> <sup>2</sup>	0.0711	1	0.0711	813.71	< 0.0001	significant
<i>B</i> <sup>2</sup>	0.0016	1	0.0016	18.35	0.0078	significant
<i>C</i> <sup>2</sup>	0.0007	1	0.0007	7.87	0.0377	significant
Residual	0.0004	5	0.0001			
Lack of Fit	0.0002	1	0.0002	2.98	0.1593	not significant
Pure Error	0.0003	4	0.0001			
Cor. Total	0.2255	14				

To assess the results, regression analysis was performed on the data in Table 4 using the quadratic equation:

$$\text{Triacetin selectivity} = 3.07203 - 0.071454A - 0.014382B - 0.156842C + 0.000166AB + 0.000034AC + 0.024157BC + 0.000427A^2 - 0.002306B^2 - 0.009443C^2 \quad (3)$$

Figure 7 shows the predicted vs. actual values for the triacetin selectivity. Almost all the points of the actual values lie on the formulated predicted line. The lack of fit test was non-significant, indicating that the model can accurately predict triacetin selectivity within the specified range of factors.

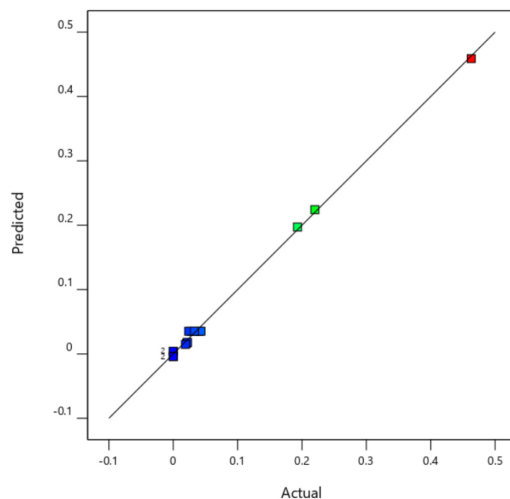


Figure 7. Predicted vs. actual values for the triacetin selectivity

Based on the p-value in **Table 4**, the significant model terms are temperature ( $A$ ), combination molar ratio and catalyst loading ( $BC$ ), enhanced temperature ( $A^2$ ), enhanced molar ratio ( $B^2$ ), and enhanced catalyst loading<sup>2</sup> ( $C^2$ ). The higher temperature will impact the selectivity of triacetin [34]. It has also been proven based on the graphs in **Figures 8a** and **8b**; as can be seen, the higher the reaction temperature, the higher the triacetin selectivity.

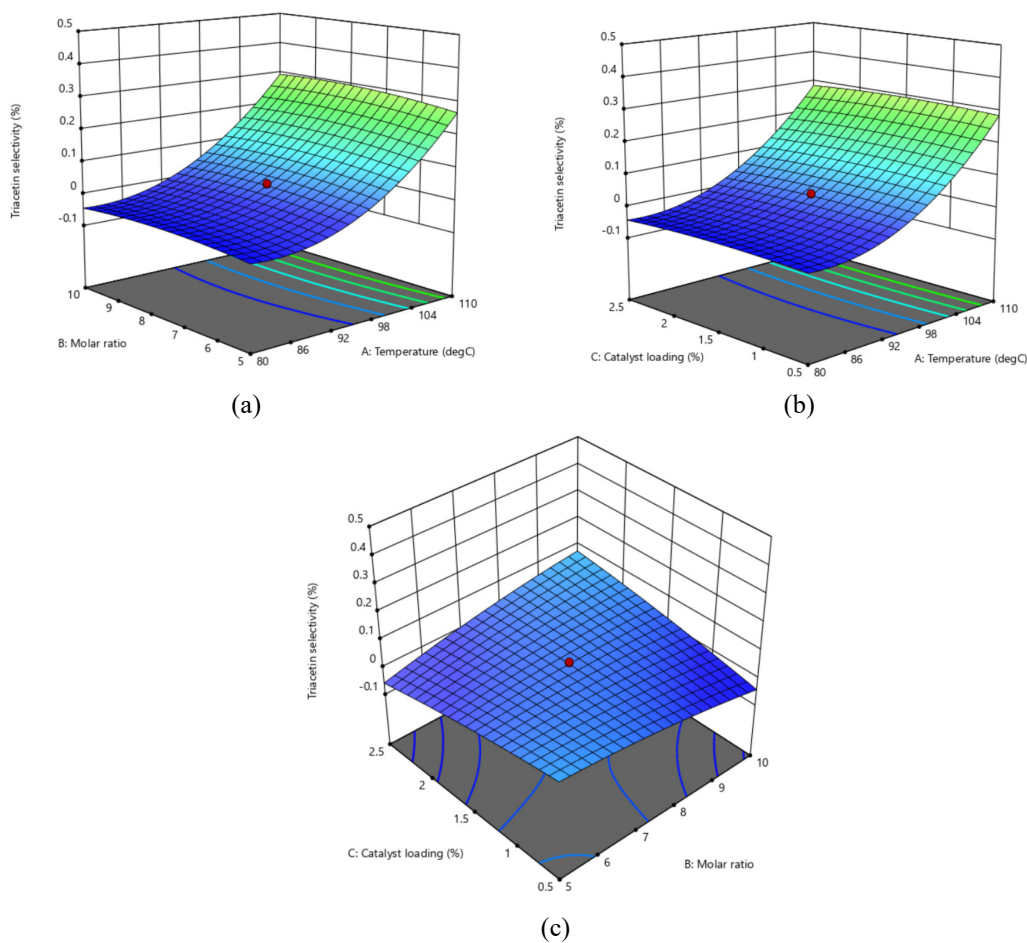


Figure 8. Impacts on triacetin selectivity: effect of temperature [°C] and molar ratio (a); effect of catalyst loading [%] and temperature [°C] (b); effect of catalyst loading [%] and molar ratio on triacetin selectivity (c)

The quadratic model was shown to be the best-fitted model for conceptualising the impacts of the parameters for the second response, which is the conversion of glycerol. **Table 5** displays a summary of the analysis of variance for the glycerol conversion regression model. The model is significant, as shown by the Model F-value of 411.92; it might occur due to noise only 0.01% of the time. Important model terms with p-values less than 0.0500 include temperature (*A*), the molar ratio (*B*), and the molar ratio & catalyst loading (*BC*). The lack of fit was not significant compared to the pure error (F-value of 0.0569). A significant Lack of Fit F-value has an 82.32% chance of being caused by noise, indicating a solid model. The discrepancy between the Predicted  $R^2$  of 0.9960 and the Adjusted  $R^2$  of 0.9758 is less than 0.2, i.e., in fair agreement.

Table 5. Analysis of variance for the regression model for glycerol conversion

Source	Sum of Squares	df	Mean Square	F-value	p-value	
Model	0.0430	9	0.0048	411.92	< 0.0001	significant
<i>A</i> – Temperature	0.0010	1	0.0010	82.67	0.0003	significant
<i>B</i> – Molar ratio	0.0148	1	0.0148	1280.21	< 0.0001	significant
<i>C</i> – Catalyst loading	0.0012	1	0.0012	104.28	0.0002	significant
<i>AB</i>	0.0006	1	0.0006	48.22	0.0010	significant
<i>AC</i>	0.0000	1	0.0000	1.64	0.2570	not significant
<i>BC</i>	0.0028	1	0.0028	245.61	< 0.0001	significant
<i>A</i> <sup>2</sup>	0.0003	1	0.0003	27.88	0.0032	significant
<i>B</i> <sup>2</sup>	0.0000	1	0.0000	1.65	0.2551	
<i>C</i> <sup>2</sup>	0.0009	1	0.0009	75.74	0.0003	significant
Residual	0.0001	5	0.0000			
Lack of Fit	8.133E-07	1	8.133E-07	0.0569	0.8232	not significant
Pure Error	0.0001	4	0.0000			
Cor. Total	0.0430	14				

Eq. (4) depicts the final empirical models of the proposed quadratic model in terms of the three real variable components. The negative signs in front of the phrases imply antagonistic effects, whereas the positive marks indicate synergistic effects [35].

$$\text{Glycerol conversion} = 95.57119 + 0.009534A + 0.093139B + 0.044304C - 0.000446AB + 0.000205AC - 0.015093BC - 0.000029A^2 - 0.000252B^2 + 0.010669C^2 \quad (4)$$

**Figure 9** shows that the points were scattered near the predicted line. The R-squared value is 0.9862, and the lack of fit test was also found to be non-significant, indicating that the model can accurately predict glycerol conversion within the specified range of factors.

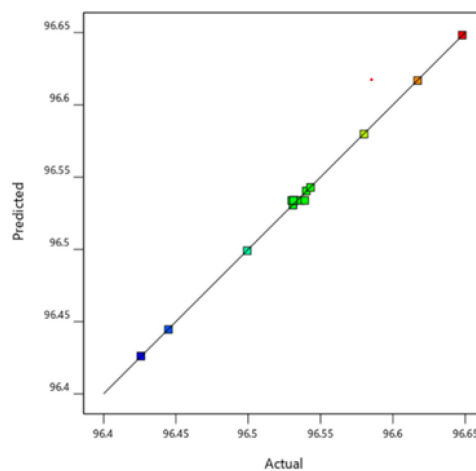


Figure 9. Predicted vs. actual values for the glycerol conversion

By referring to the p-value in **Table 5**, the significant model terms are temperature ( $A$ ), the molar ratio ( $B$ ), catalyst loading ( $C$ ), temperature & catalyst loading ( $AC$ ), molar ratio & catalyst loading ( $BC$ ), squared temperature ( $A^2$ ), and squared catalyst loading ( $C^2$ ). The higher temperature and molar ratio influenced the glycerol conversion. Besides, this has also been proven based on the graphs in **Figures 10a** and **Figures 10b**; as can be seen, the higher the reaction temperature, the higher the percentage of triacetin selectivity.

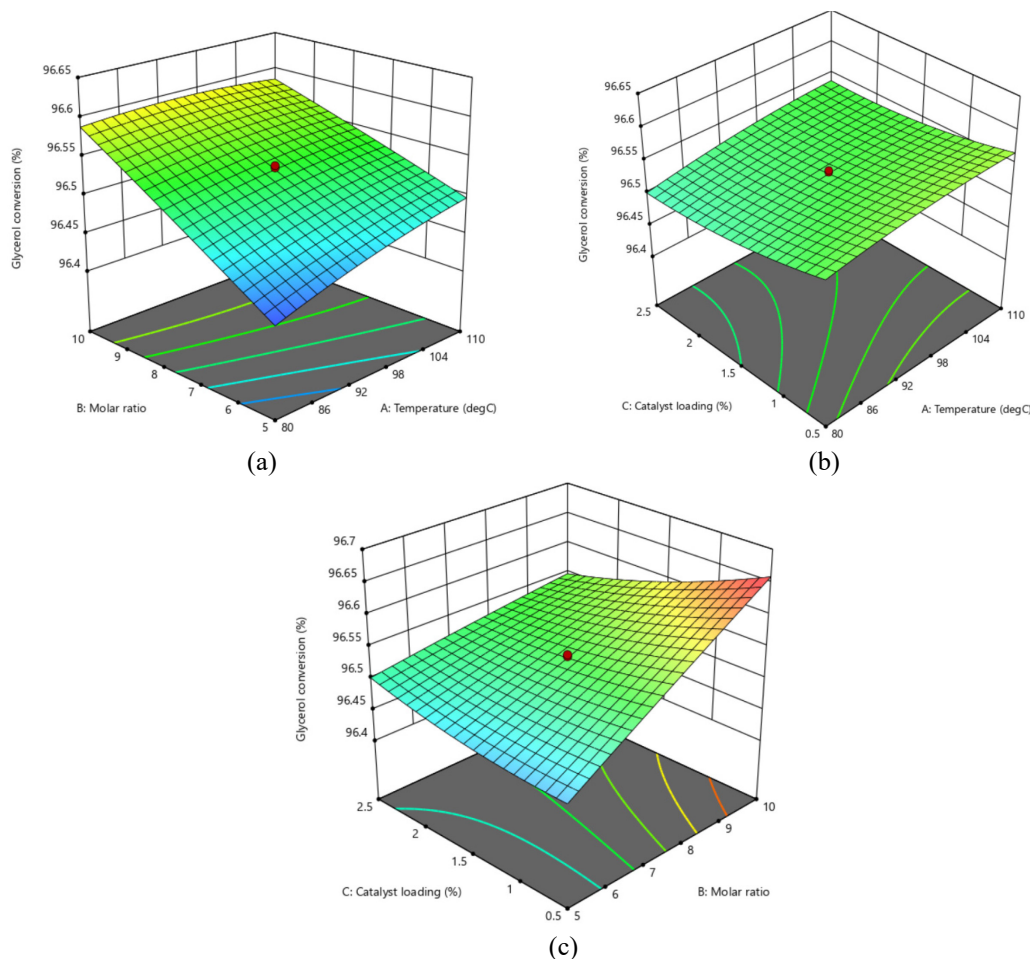


Figure 10. Impacts on glycerol conversion: effect of temperature [ $^{\circ}\text{C}$ ] and molar ratio (a); effect of catalyst loading [%] and temperature [ $^{\circ}\text{C}$ ] (b); effect of catalyst loading [%] and molar ratio (c)

### Effect of reaction temperatures

The effect of reaction temperature (80 $^{\circ}\text{C}$  to 110 $^{\circ}\text{C}$ ) on glycerol conversion and product selectivity was investigated at a 90 min reaction time. The interaction between reactants and catalysts increases as the temperature increases. Moreover, an increase in temperature reduces the viscosity of glycerol and enhances its solubility [36]. It can also enhance the diffusion of reactants and products in and out of the active sites. It is also known that high triacetin selectivity and glycerol conversion are achieved at high temperatures as it is an endothermic process [37].

The triacetin selectivity increased drastically as the temperature increased at the expense of monoacetin and diacetin. It shows the necessity of temperature to convert monoacetin and diacetin to triacetin efficiently. Triacetin and glycerol conversion selectivity were best at 116  $^{\circ}\text{C}$  and 110  $^{\circ}\text{C}$ , respectively. Nevertheless, further increments in temperature above 110  $^{\circ}\text{C}$  lead to decreased selectivities due to the reduced accessibility of acetic acid, which causes it to evaporate at a higher rate [9]. Moreover, collisions between atoms increase at higher reaction temperatures [36].

### Effect of reactant molar ratio

Acetylation of glycerol can be enhanced by instigating one of the reactants in excess. Three moles of acetic acid and one mole of glycerol are needed to produce one mole of triacetin. The conversion of glycerol was increased by increasing the glycerol/acetic acid molar ratio up to 1:10. As glycerol acetylation is a reversible reaction, the surplus of acetic acid in the reaction mixture improves the reaction towards the conversion of glycerol but not the triacetin selectivity. The optimum conversion of 96.64% was attained at the glycerol/acetic acid ratio of 1:10. Additionally, excessive usage of acetic acid in the acetylation of glycerol reduces the time required to accomplish equilibrium. It offers more acetylation agents that produce triacetin with further acetylation. Hence, it can be deduced that an increase in the molar ratio between acetic acid and glycerol will increase glycerol conversion [36]. Though it must be noted that a further increase in molar ratios does not cause any changes in triacetin selectivity or glycerol conversion, more acetic acid molecules would attach to the same active sites at Pd/AC [9].

### Effect of catalyst loading

As the Pd/AC loading increases, the selectivity of triacetin and the conversion of glycerol improve due to the availability of more active sites on Pd/AC [38]. Yet, the reaction efficiency declines if the Pd/AC loading is increased beyond a certain point because the particles start to aggregate, reducing the access of reactants to the Pd/AC catalyst and impeding the transfer rates to active sites within the aggregates. Using a moderate catalyst amount is advisable to achieve high glycerol conversion and selectivity towards triacetin [9].

### The role of triacetin in the circular economy

The production of glycerol from biodiesel, using either vegetable oil or animal fat, results in oxygenated additions that are biodegradable, non-toxic, and renewable. Three classes of oxygenated additives can be distinguished: acetins, glycerol ethers, and glycerol formal. These gasoline additives made from the conversion of glycerol could replace traditional petroleum-based additives like ethyl tert-butyl ether and methyl tert-butyl ether. Fuel additives are often used to enhance engine performance and reduce various engine components' corrosion [39].

Moreover, employing triacetin as a fuel additive can lead to significant reductions, such as up to 75% in hydrocarbon (HC) emissions, around 10% in carbon dioxide (CO<sub>2</sub>) emissions, 50% in carbon monoxide (CO) emissions, and 28 to 29% in nitrogen oxide (NO) emissions, compared to diesel and non-blended biodiesel [40]. This finding showed another positive outcome in applying blended biodiesel with glycerol-based fuel additives. It can also improve biodiesel's economics by reducing its manufacturing costs, in line with the circular economy and net-zero carbon emission frameworks.

The environment, raw material supply security, competitiveness, innovation, economic growth acceleration, and creation of jobs may all benefit from a more circular economy. Additionally, customers will receive more innovative and long-lasting products, which will enhance their quality of life and help them save money in the long run [41].

## CONCLUSIONS

The Pd/AC catalyst enhanced the efficiency of glycerol acetylation under microwave irradiation, responding to the independent factors. The temperature of 110 °C, the glycerol and acetic acid molar ratio of 1:10, and the catalyst load of 0.718 wt% were found to be the best conditions for generating high triacetin selectivity and glycerol conversion after utilising RSM to optimise the reaction parameters. The increase in reaction temperature is one of the parameters that can increase triacetin selectivity.

The biodiesel industry is growing with increasing demand and produces a surplus of glycerol that can be used as a fuel additive. Also, the availability of a suitable and active green catalyst at a low cost will enhance the production of acetins, especially triacetin.

## ACKNOWLEDGMENTS

The authors would like to acknowledge the conferment of HICoE support from the Ministry of Higher Education Malaysia to the HICoE-Centre for Biofuel and Biochemical Research and the funding support from Yayasan UTP Internal Fund (No. 015LC0-201). The research facilities' support from the Centre for Biofuel and Biochemical Research at Universiti Teknologi PETRONAS is greatly appreciated.

## NOMENCLATURE

### Abbreviations

ANOVA	Analysis of variance
CCD	Central composite design
FESEM-EDS	Field emission scanning electron microscopy coupled with energy-dispersive spectroscopy
FTIR	Fourier transform infrared spectrometry
GC	Glycerol conversion
GC-FID	Gas chromatography with flame ionisation detection
HPLC	High-performance liquid chromatography
NH <sub>3</sub> -TPD	Ammonia-temperature programmed desorption analysis
Pd/AC	Palladium on activated carbon catalyst
RSM	Response surface methodology
TGA	Thermogravimetric analysis
TS	Triacetin selectivity
XRD	X-ray diffraction

## REFERENCES

1. BP, "Statistical review of world energy 2012," 2012. <http://www.bp.com>, [Accessed 15-April-2021].
2. M. Höök and T. Xu, "Depletion of fossil fuels and anthropogenic climate change – a review," *Energy Policy*, vol. 52, pp. 797–809, 2013, <https://doi.org/10.1016/j.enpol.2012.10.046>.
3. A. G. Wahab, "Biofuels Annual," Report, MY2019-0009, Kuala Lumpur, 2019.
4. U. I. Nda-Umar, I. Ramli, E. N. Muhamad, Y. H. Taufiq-Yap, and N. Azri, "Synthesis and characterisation of sulfonated carbon catalysts derived from biomass waste and its evaluation in glycerol acetylation," *Biomass Convers Biorefin*, 2020, <https://doi.org/10.1007/s13399-020-00784-0>.
5. L. Zhou, E. Al-Zaini, and A. A. Adesina, "Catalytic characteristics and parameters optimisation of the glycerol acetylation over solid acid catalysts," *Fuel*, vol. 103, pp. 617–625, 2013, <https://doi.org/10.1016/j.fuel.2012.05.042>.
6. ResearchAndMarkets, "Global Glycerol Industry (2020 to 2027) - Market Trends and Drivers," <https://www.businesswire.com/news/home/20210115005399/en/Global-Glycerol-Industry-2020-to-2027---Market-Trends-and-Drivers---ResearchAndMarkets.com>, [Accessed: 15-January-2021].
7. S. Wamucii, "Malaysia glycerol export quantities," 2022, <https://www.selinawamucii.com/insights/prices/malaysia/glycerol/>, [Accessed: 15-January-2021].
8. Z. Mufrodi, Rochmadi, Sutijan, and A. Budiman, "Synthesis acetylation of glycerol using batch reactor and continuous reactive distillation column," *Engineering Journal*, vol. 18, no. 2, pp. 29–39, 2014, <https://doi.org/10.4186/ej.2014.18.2.29>.

9. R. M. Kulkarni et al., "Kinetic studies on the synthesis of fuel additives from glycerol using CeO<sub>2</sub>-ZrO<sub>2</sub> metal oxide catalyst," *Biofuel Research Journal*, vol. 7, no. 1, pp. 1100–1108, 2020, <https://doi.org/10.18331/BRJ2020.7.1.2>.
10. P. S. Kong, M. K. Aroua, W. M. A. W. Daud, H. V. Lee, P. Cognet, and Y. Pères, "Catalytic role of solid acid catalysts in glycerol acetylation for the production of bio-additives: A review," *RSC Adv*, vol. 6, no. 73, pp. 68885–68905, 2016, <https://doi.org/10.1039/c6ra10686b>.
11. H. Rastegari, H. S. Ghaziaskar, M. Yalpani, and A. Shafiei, "Development of a Continuous System Based on Azeotropic Reactive Distillation to Enhance Triacetin Selectivity in Glycerol Esterification with Acetic Acid," *Energy and Fuels*, vol. 31, no. 8, pp. 8256–8262, 2017, <https://doi.org/10.1021/acs.energyfuels.7b01068>.
12. E. M. Morais, I. B. Grillo, H. K. Stassen, M. Seferin, and J. D. Scholten, "The effect of an electron-withdrawing group in the imidazolium cation: The case of nitro-functionalised imidazolium salts as acidic catalysts for the acetylation of glycerol," *New Journal of Chemistry*, vol. 42, no. 13, pp. 10774–10783, 2018, <https://doi.org/10.1039/c8nj02520g>.
13. N. Hidayati, R. P. Sari, and H. Purnama, "Catalysis of glycerol acetylation on solid acid catalyst: a review," *Jurnal Kimia Sains dan Aplikasi*, vol. 23, no. 12, pp. 414–423, Jan. 2021, <https://doi.org/10.14710/jksa.23.12.414-423>.
14. S. Karnjanakom, P. Maneechakr, C. Samart, and G. Guan, "Ultrasound-assisted acetylation of glycerol for triacetin production over green catalyst: A liquid biofuel candidate," *Energy Convers Manag*, vol. 173, no. June, pp. 262–270, 2018, <https://doi.org/10.1016/j.enconman.2018.07.086>.
15. M. Marwan, E. Indarti, D. Darmadi, W. Rinaldi, D. Hamzah, and T. Rinaldi, "Production of triacetin by microwave assisted esterification of glycerol using activated natural zeolite," *Bulletin of Chemical Reaction Engineering & Catalysis*, vol. 14, no. 3, pp. 672–677, 2019, <https://doi.org/10.9767/bcrec.14.3.4250.672-677>.
16. S. Magar, G. T. Mohanraj, S. K. Jana, and C. V. Rode, "Synthesis and characterisation of supported heteropoly acid: Efficient solid acid catalyst for glycerol esterification to produce biofuel additives," *Inorganic and Nano-Metal Chemistry*, vol. 50, no. 11, pp. 1157–1165, 2020, <https://doi.org/10.1080/24701556.2020.1737817>.
17. G. A. Bedogni, M. D. Acevedo, F. Aguzín, N. B. Okulik, and C. L. Padró, "Synthesis of bioadditives of fuels from biodiesel-derived glycerol by esterification with acetic acid on solid catalysts," *Environmental Technology (United Kingdom)*, vol. 39, no. 15, pp. 1955–1966, 2018, <https://doi.org/10.1080/09593330.2017.1345986>.
18. S. Bewana, M. Joe Ndolomingo, R. Meijboom, and N. Bingwa, "Cobalt oxide promoted tin oxide catalysts for highly selective glycerol acetalisation reaction," *Inorg Chem Commun*, vol. 128, no. March, p. 108578, 2021, <https://doi.org/10.1016/j.inoche.2021.108578>.
19. R. Jothi Ramalingam, J. N. Appaturi, T. Pulingam, H. A. Al-Lohedan, and D. M. Aldhayan, "In-situ incorporation of ruthenium/copper nanoparticles in mesoporous silica derived from rice husk ash for catalytic acetylation of glycerol," *Renew Energy*, vol. 160, pp. 564–574, 2020, <https://doi.org/10.1016/j.renene.2020.06.095>.
20. U. I. Nda-Umar, I. Ramli, E. N. Muhamad, N. Azri, and Y. H. Taufiq-Yap, "Optimisation and Characterisation of Mesoporous Sulfonated Carbon Catalyst and Its Application in Modeling and Optimisation of Acetin Production," *Molecules*, vol. 25, no. 22, pp. 1–23, 2020, <https://doi.org/10.3390/molecules25225221>.
21. P. U. Okoye, A. Z. Abdullah, and B. H. Hameed, "Synthesis of oxygenated fuel additives via glycerol esterification with acetic acid over bio-derived carbon catalyst," *Fuel*, vol. 209, no. July, pp. 538–544, 2017, <https://doi.org/10.1016/j.fuel.2017.08.024>.
22. M. R. A. Arcanjo, I. J. Silva, E. Rodríguez-Castellón, A. Infantes-Molina, and R. S. Vieira, "Conversion of glycerol into lactic acid using Pd or Pt supported on carbon as catalyst,"

- Catalysis Today, vol. 279, pp. 317–326, 2017, <https://doi.org/10.1016/j.cattod.2016.02.015>.
23. M. Bartoli, C. Zhu, M. Chae, and D. C. Bressler, "Glycerol acetylation mediated by thermally hydrolysed biosolids-based material," *Catalysts*, vol. 10, no. 1, 2020, <https://doi.org/10.3390/catal10010005>.
  24. T. G. J. and R. G. C. G. G. Wildgoose, H. C. Leventis, I. J. C. A. Davies, N. S. Lawrence, L. Jiang, "Graphite powder derivatised with poly-l-cysteine using 'building-block' chemistry—a novel material for the extraction of heavy metal ions," *Journal of Material Chemistry*, vol. 15, no. 24, pp. 2375–2382, 2005, <https://doi.org/10.1039/b504170h>.
  25. C. Hsieh and H. Teng, "Influence of mesopore volume and adsorbate size on adsorption capacities of activated carbons in aqueous solutions," *Carbon N Y*, vol. 38, no. 6, pp. 863–869, 2000, [https://doi.org/10.1016/S0008-6223\(99\)00180-3](https://doi.org/10.1016/S0008-6223(99)00180-3).
  26. A. Namdeo, S. M. Mahajani, and A. K. Suresh, "Palladium catalysed oxidation of glycerol - Effect of catalyst support," *J Mol Catal A Chem*, vol. 421, pp. 45–56, 2016, <https://doi.org/10.1016/j.molcata.2016.05.008>.
  27. D. Hamzah, T. Rinaldi, M. Marwan, and W. Rinaldi, "Synthesis of Triacetin Catalyzed by Activated Natural Zeolite Under Microwave Irradiation," *Jurnal Bahan Alam Terbarukan*, vol. 8, no. 1, pp. 01–07, 2019, <https://doi.org/10.15294/jbat.v8i1.14028>.
  28. L. P. Dill, D. M. Kochepka, A. Melinski, F. Wypych, and C. S. Cordeiro, "Microwave-irradiated acetylation of glycerol catalysed by acid activated clays," *Reaction Kinetics, Mechanisms and Catalysis*, vol. 127, no. 2, pp. 991–1004, 2019, <https://doi.org/10.1007/s11144-019-01594-w>.
  29. C. Tu and S. Cheng, "Ceria-modified palladium/activated carbon as a high-performance catalyst for crude caprolactam hydrogenation purification," *ACS Sustain Chem Eng*, vol. 2, no. 4, pp. 629–636, 2014, <https://doi.org/10.1021/sc400501w>.
  30. B. Stephen and L. Linda, "Agilent Hi-Plex Columns for Carbohydrates, Alcohols, and Acids," Agilent Technologies Inc.
  31. B. Qi, L. Di, W. Xu, and X. Zhang, "Dry plasma reduction to prepare a high performance Pd/C catalyst at atmospheric pressure for CO oxidation," *J Mater Chem A Mater*, vol. 2, no. 30, pp. 11885–11890, 2014, <https://doi.org/10.1039/c4ta02155j>.
  32. S. Kumar, N. Viswanadham, S. K. Saxena, A. Selvamani, J. Diwakar, and A. H. Al-Muhtaseb, "Single-pot template-free synthesis of a glycerol-derived C-Si-Zr mesoporous composite catalyst for fuel additive production," *New Journal of Chemistry*, vol. 44, no. 20, pp. 8254–8263, 2020, <https://doi.org/10.1039/d0nj00523a>.
  33. N. Ya'Aini, A. Pillay Al Gopala Krishnan, and A. Ripin, "Synthesis of activated carbon doped with transition metals for hydrogen storage," *E3S Web of Conferences*, vol. 90, 2019, <https://doi.org/10.1051/e3sconf/20199001016>.
  34. R. Usman Idris Nda-Umar, E. N. Muhamad, N. Azri, and Y. H. Taufiq-Yap, "Optimisation and Characterisation of Mesoporous Sulfonated Carbon Catalyst and Its Application in Modeling and Optimisation of Acetin Production," *Molecules*, vol. 25, p. 5521, 2020, <https://doi.org/10.3390/molecules25225221>.
  35. Welty, G. L. Rorrer, and D. G. Foster, *Fundamentals of Momentum, Heat, and Mass Transfer*. Wiley, 2014.
  36. N. Hidayati, R. P. Sari, and H. Purnama, "Catalysis of glycerol acetylation on solid acid catalyst: a review," *Jurnal Kimia Sains dan Aplikasi*, vol. 23, no. 12, pp. 414–423, 2021, <https://doi.org/10.14710/jksa.23.12.414-423>.
  37. U. I. Nda-Umar et al., "Organosulfonic acid-functionalised biomass-derived carbon as a catalyst for glycerol acetylation and optimisation studies via response surface methodology," *J Taiwan Inst Chem Eng*, vol. 118, pp. 355–370, 2021, <https://doi.org/10.1016/j.jtice.2020.12.021>.



38. M. S. Khayoon and B. H. Hameed, "Acetylation of glycerol to biofuel additives over sulfated activated carbon catalyst," *Bioresource Technology*, vol. 102, no. 19, pp. 9229–9235, 2011, <https://doi.org/10.1016/j.biortech.2011.07.035>.
39. A. Cornejo, I. Barrio, M. Campoy, J. Lázaro, and B. Navarrete, "Oxygenated fuel additives from glycerol valorisation. Main production pathways and effects on fuel properties and engine performance: A critical review," *Renewable and Sustainable Energy Reviews*, vol. 79, pp. 1400–1413, Nov. 2017, <https://doi.org/10.1016/j.rser.2017.04.005>.
40. P. V. Rao, "Role of Triacetin additive in the performance of single cylinder D I diesel engine with COME biodiesel," *International Journal of Advanced Engineering Research and Science*, vol. 5, no. 9, pp. 253–260, 2018, <https://doi.org/10.22161/ijaers.5.9.28>.
41. European Parliament, "Circular economy: definition, importance and benefits," [https://www.europarl.europa.eu/pdfs/news/expert/2015/12/story/20151201STO05603/20151201STO05603\\_en.pdf](https://www.europarl.europa.eu/pdfs/news/expert/2015/12/story/20151201STO05603/20151201STO05603_en.pdf), [Accessed: 25-June-2022].



Paper submitted: 09.04.2023

Paper revised: 12.07.2023

Paper accepted: 14.07.2023